Journal of Physics: Conference Series **572** (2014) 012009 doi:10.1088/1742-6596/572/1/012009

Charge transfer in cold collisions of rubidium atoms with calcium and ytterbium ions

S A Yakovleva[1], A K Belyaev[1] and A A Buchachenko[2]

[1] Department of Theoretical Physics and Center for Advanced Study, Herzen University, St. Petersburg 191186, Russia

[2] Department of Chemistry, M.V. Lomonosov Moscow State University, Moscow 119991, Russia

Abstract. Low-energy collisions of the Ca and Yb cations with Rb atoms are investigated theoretically using accurate *ab initio* potential energy curves and coupling matrix elements to elucidate the dominant charge transfer mechanisms. The cross sections calculated at collision energies above 10^{-5} cm^{-1} exhibit the features typical to Langevin ion-atom collision regime, including a rich structure associated with the centrifugal barrier tunnelling (orbiting) resonances. It is shown that the dominant process in Yb^+ + Rb collisions is the radiative charge transfer, while in the case of Ca^+ + Rb collisions nonadiabatic transitions due to spin-orbit coupling dominate. Theoretical results are in a good agreement with available experimental data.

1. Introduction

With the development of the hybrid traps, which combine laser-cooled atomic ions stored in a radio-frequency trap and ultracold or statistically condensed neutral atoms in a magneto-optical trap, study of the ion-neutral reactions in the energy range between 1 mK and 1 K (usually termed as "cold" conditions) has recently become possible. Due to strong attractive induction interaction, cold ion-neutral collisions do not follow quantum regime being closer to "statistical" Langevin multiple partial wave picture. The effects of the orbiting resonances inherent to Langevin regime on charge transfer, a prototypical process for ion-molecular reaction, can only be understood theoretically since the micromotions of the trapped ions limit experimental collision energy resolution. The same is true for radiative-assisted processes, which are masked experimentally by the cooling laser field. Present work adresses these issues for the charge-transfer dynamics in cold collisions of the Yb^+ ions with Rb atom, studied recently using the hybrid trap technique [1], as well as the Ca^+ + Rb cold collisions [2], which, despite apparent similarity, exhibit quite distinct nonadiabatic charge transfer mechanism.

2. Interaction and dynamics

2.1. Ab initio data

Potential energy curves and coupling matrix elements used here were obtained *ab initio* under the scalar-relativistic approximation as described in great detail in [3, 4]. Those relevant to Yb^+ + Rb charge transfer are shown in Fig.1 (upper panel). The $A^1\Sigma^+$ state represents the initial channel, from which transition may occur to the ground $X^1\Sigma^+$ state. Nonadiabatic coupling matrix elements (NACMEs), responsible for nonradiative charge transfer mechanism, arise from

Content from this work may be used under the terms of the Creative Commons Attribution 3.0 licence. Any further distribution of this work must maintain attribution to the author(s) and the title of the work, journal citation and DOI.
Published under licence by IOP Publishing Ltd

the first- and second-order radial couplings and the second-order rotational couplings, presented in lower panel of the same figure.

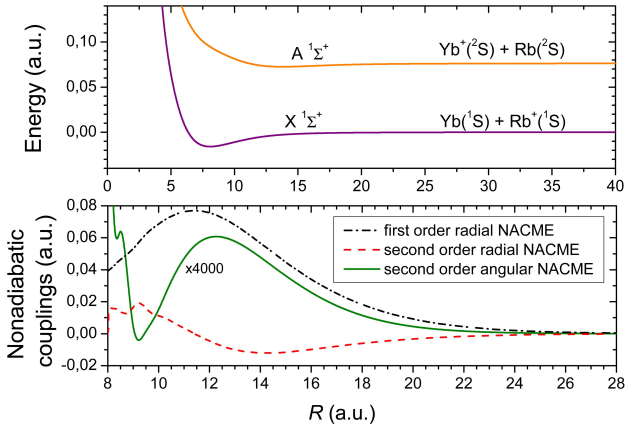


Figure 1. Potential energy curves and coupling matrix elements for $Yb^+(^2S) + Rb(^2S) \rightarrow Yb(^1S) + Rb^+(^1S)$ charge transfer process.

2.2. Nuclear dynamics

The nonadiabatic nuclear dynamics was studied within the formalism of the standard adiabatic (Born-Oppenheimer) approach described, for example, in Refs. [5, 6, 7, 8]. Due to the large energy splitting and small values of coupling matrix elements, the nonadiabatic transition probabilities are expected to be small at low collision energies, and the system of the coupled channel equations [7, 8] can be solved within the perturbation theory as shown in [5, 9].

The probabilities for a nonadiabatic transitions $i \rightarrow f$ represented by the unperturbed (elastic) scattering radial wave functions $F^{el}_{i(f)}(R)$ for the channel $i(f)$, respectively, are given by the following formulae:

$$P^{rad}_{if} = \frac{1}{4}\left|\int_0^\infty \langle\psi_{i\Lambda}|\frac{\partial}{\partial R}|\psi_{f\Lambda}\rangle\left[F^{el}_{i\Lambda}\frac{dF^{el}_{f\Lambda}}{dR} - F^{el}_{f\Lambda}\frac{dF^{el}_{i\Lambda}}{dR}\right]dR\right|^2 \quad (1)$$

for the radial couplings and

$$P^{ang}_{if} = \left|\int_0^\infty \frac{1}{R^2}\left[F^{el}_{i\Lambda}\langle\psi_{i\Lambda}|L_x^2 + L_y^2|\psi_{f\Lambda}\rangle F^{el}_{f\Lambda}\right]dR\right|^2, \quad (2)$$

for the angular coupling. In contrast to Yb^+ + Rb case, where the initial and final charge transfer channels are not coupled by spin-orbit (SO) interaction, it had to be considered for Ca^+ + Rb collisions. The corresponding probability is

$$P^{so}_{if} = \left|2\mu\int_0^\infty \left[F^{el}_{i\Lambda}\langle\psi_{i\Lambda}|\hat{H}^{so}|\psi_{f\Lambda'}\rangle F^{el}_{f\Lambda'}\right]dR\right|^2, \quad (3)$$

where μ is the reduced nuclear mass of the colliding partners.

The nonradiative charge transfer cross sections are computed as a sum over the total angular momentum quantum number J

$$\sigma_{if}(E) = \frac{\pi\hbar^2 p_i^{stat}}{2\mu E}\sum_{J=0}^{J_{max}} P_{if}(J,E)(2J+1), \quad (4)$$

where p_i^{stat} is the statistical probability for population of the initial channel i.

The dipole coupling between molecular states induces radiative charge transfer mechanism. An expression for the total radiative cross section follows from the optical potential approach [10, 11, 12, 13]. Being combined with the distorted wave approximation, it reads [10]

$$\sigma_{if}^{R}(E) = \frac{\pi}{2\mu E} p_i^{stat} \sum_J (2J+1)\{1 - \exp[-4\eta_J(E)]\} \tag{5}$$

with

$$\eta_J(E) = \frac{2\pi}{3}\sqrt{\frac{\mu}{2E}}\alpha^3 \int_0^\infty F_i^{J,E} d_{if}^2(R)[U_i - U_f]^3 F_i^{J,E} dR, \tag{6}$$

where $F_i^{J,E}$ is the unperturbed (elastic) scattering radial wave function, d_{if} is the transition dipole matrix element and $U_{i(f)}$ denotes adiabatic potential.

3. Results and conclusions

Cross sections for radiative and nonradiative charge transfer in $Yb^+ + Rb$ collisions are shown in Fig.2. Evidently, the latter gives negligible contribution to the charge transfer due to large adiabatic splitting and weak interaction of the $A^1\Sigma^+$ and $X^1\Sigma^+$ states. At the same time, it is worthy of noting that all cross sections exhibit the same resonance structure. Partial wave analysis demonstrate that it entirely corresponds to the orbiting, strong narrow resonances – to the tunneling deep under the centrifugal barriers and weak broad features – to the capture slightly below or above the barriers. Detailed analysis of some resonances [14] clearly shows the occurrence of dynamical trapping of the colliding partners in the entrance channel, causing a correspondingly marked increase of the non-adiabatic transition probabilities.

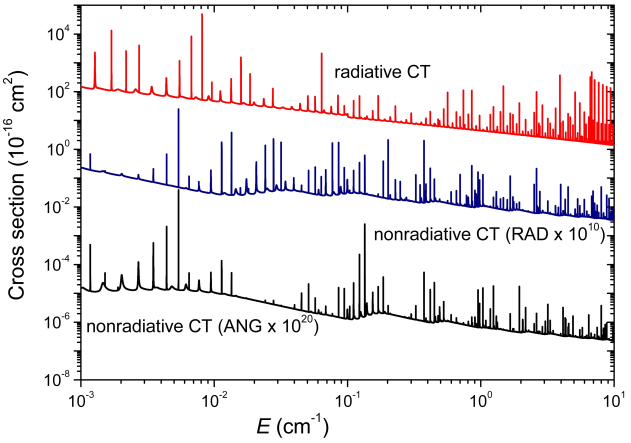


Figure 2. Energy-dependent cross sections for the $A^1\Sigma^+ \rightarrow X^1\Sigma^+$ process in $Yb^+ + Rb$ collisions. The uppermost (red) trace shows the radiative cross section. The second from the top (blue) trace represents nonradiative cross section due to the radial NACMEs (multiplied by 10^{10}). The bottom (black) trace depicts the non-radiative cross section due to the angular NACME (multiplied by 10^{20}).

As far as the kinetic energy in a hybrid trap is controlled by ion micromotions, it is convenient to introduce energy-dependent rate coefficient as $R(E) = \sqrt{2E/\mu}\,\sigma_{AX}^{R}(E)$. It is shown in Fig.3 together with the experimental data. Note that the resonance component gives about 10% of the total rate. The mean theoretical rate coefficient is in good agreement with the measured one. It has been demonstrated that account for SO interaction that modifies the potential energy curve for initial channel further improves the coincidence with experiment [4].

In contrast, detailed investigation of $Ca^+ + Rb$ collisions [3, 14] showed that the $Ca^+(^2S) + Rb(^2S) \rightarrow Ca(^3P) + Rb^+(^1S)$ charge transfer at very low collision energies proceeds by the non-radiative mechanism. The states involved, $A^1\Sigma$ and $b^3\Pi$, are coupled by the SO matrix element, whereas two crossings of the corresponding adiabatic potentials further facilitate the nonadiabatic charge transfer process. Its cross sections, shown in Fig.4, indicate that Langevin

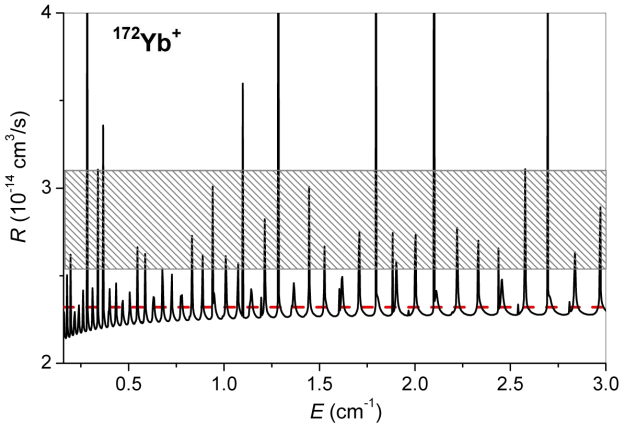


Figure 3. Energy-dependent rate coefficient for the radiative transfer in the $^{172}Yb^+$ + Rb collisions. Horizontal dashed line represents the mean value, shaded area – the experimental error bars [1].

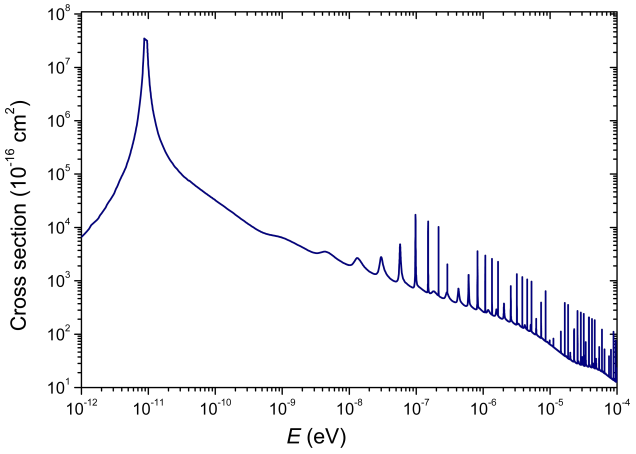


Figure 4. The calculated cross section for the $Ca^+(^2S)$ + $Rb(^2S)$ → $Ca(^3P)$ + $Rb^+(^1S)$ nonradiative charge transfer process as a function of the collision energy.

regime onsets at collision energy above 10^{-5} cm^{-1}. The calculated rate coefficient for Ca^++Rb collisions is equal to 3.5×10^{-12} cm^3/s at the temperature $T = 2$ K and in good agreement with the experimental data 2×10^{-12} cm^3/s reported in [2].

To conclude, charge-transfer collisions at the energies typical to hybrid traps follow Langevin regime with its inherent rich orbiting resonance structure. This structure tend to enhance the rate of inelastic processes. The mechanism of charge transfer may vary from system to system being determined by the structure of adiabatic potential energy curves and magnitude of the couplings. The dominant mechanisms in the treated cold collisions are different: It is the radiative charge transfer in Yb^+ + Rb collisions, while the main mechanism in Ca^+ + Rb collisions corresponds to the nonradiative charge transfer. Spin-orbit interactions are essential for a quantitative description of the cold charge transfer dynamics.

Acknowledgments

We acknowledge financial support from the Russian Foundation for Basic Research (grants 11-03-00081 and 13-03-00163).

References

[1] Zipkes C, Palzer S, Ratschbacher L, Sias C and Köhl M 2010 *Phys. Rev. Lett.* **105** 133201
[2] Hall F H J, Eberle P, Hegi G, Willitsch S, Raoult M, Aymar M and Dulieu O 2013 *Mol. Phys.* **111** 2020–32
[3] Tacconi M, Gianturco F A and Belyaev A K 2011 *Phys. Chem. Chem. Phys.* **13** 19156
[4] Sayfutyarova E R, Buchachenko A A, Yakovleva S A and Belyaev A K 2013 *Phys. Rev.* A **87** 052717
[5] Mott N F and Massey H S W 1949 *The Theory of Atomic Collisions* (Oxford: Clarendon Press)

[6] Macias A and Riera A 1982 *Phys.Rep.* **90**, 299
[7] Grosser J 1986 *Z. Phys.* D **3** 39
[8] Belyaev A K, Egorova D, Grosser J and Menzel T 2001 *Phys. Rev.* A **64** 052701
[9] Belyaev A K 2007 *Eur. Phys. J.* D **44** 497
[10] Zygelman B and Dalgarno A 1988 *Phys. Rev.* A **38** 1877
[11] Cohen J S and Bardsley J N 1978 *Phys. Rev.* A **18** 1004
[12] Tellinghuisen J and Julienne P S 1984 *J. Chem. Phys.* **81** 5779
[13] Gustafsson M, Antipov S V, Franz J and Nyman G 2012 *J. Chem. Phys.* **137** 104301
[14] Belyaev A K, Yakovleva S A, Tacconi M and Gianturco F A 2012 *Phys. Rev.* A **85** 042716